

Supplemental material

Alternate routes to mnm⁵s²U synthesis in Gram-positive bacteria

Marshall Jaroch^{a1}, Guangxin Sun^{b,c1}, Ho-Ching Tiffany Tsui^d, Colbie Reed^a, Jinjing Sun^{b,c}, Marko Jörg^{a,&}, Malcolm E. Winkler^d, Kelly C. Rice^a, Agnieszka Dziergowska^e, Troy A. Stich^f, Peter C. Dedon^{b,c}, Patricia C. Dos Santos^{f,2} and Valérie de Crécy-Lagard^{a,g,2}

^a Department of Microbiology and Cell Science, University of Florida, Gainesville, FL 32611;

^b Department of Biological Engineering, Massachusetts Institute of Technology, Cambridge, MA 02139

^c Singapore-MIT Alliance for Research and Technology, Singapore

^d Department of Biology, Indiana University Bloomington, Bloomington, IN, USA

^e Institute of Organic Chemistry, Lodz University of Technology, 90-924 Łódź, Poland

^f Department of Chemistry, Wake Forest University, Winston-Salem, NC, 27101, USA

^g University of Florida Genetics Institute, Gainesville, FL 32610, USA

¹ Contributed equally

² To whom correspondence may be addressed: vcrcy@ufl.edu & dossanpc@wfu.edu

& Current address Department of Pharmacology and Toxicology, Institute of Pharmaceutical and Biomedical Sciences, Johannes Gutenberg University Mainz, 55128 Mainz, Germany

Supplemental Tables

Table S1. Distribution of MnmC2, MnmC1/C2 fusions, YtqA, and instances of YtqA homologs physically clustered with YtqB.

Group Name	Tax ID	Number of Genomes	YtqA (%)	YtqA clusters w. YtqB (%)	MnmC2 (%)	MnmC1/C2 Fusion (%)	Of Those w/o MnmC (MnmC1, MnmC2, or MnmC1/C2 fusion)	
							YtqA (%)	YtqA clusters w. YtqB (%)
Acidobacteria	57723	7	0	NA	0	0	0	0
Aquificae	187857	9	89	13	78	0	100	50
Bacteroidetes	200643	106	23	13	85	0	25	6
Chlamydiae	204428	6	0	NA	0	0	0	0
Chlorobi	1090	5	0	NA	0	0	0	0
Chloroflexi	32061	5	0	NA	0	0	0	0
Cyanobacteria	1117	41	5	0	90	0	25	0
Deferribacteres	68337	5	100	40	0	0	0	0
Deinococcus-thermus	1297	6	0	NA	0	0	0	0
Bacilli	91061	67	45	80	0	0	67	36
Clostridia	186801	75	60	22	0	0	71	13
Negativicutes	909932	10	60	83	0	0	70	50
Tissierellia	1737404	8	75	17	0	0	88	13
Other Firmicutes	53420*	3	33	100	0	0	67	33
Fusobacteria	203490	6	50	0	0	0	50	0
Mollicutes	31969	14	14	50	0	0	14	7
Planctomycetes	112	14	29	0	0	0	29	0
Alphaproteobacteria	28211	150	0	NA	31	10	0	0
Betaproteobacteria	28216	99	12	33	4	65	3	0
Deltaproteobacteria	28221	32	47	47	19	0	69	27
Epsilonproteobacteria	3031852	12	67	25	75	8	3	0
Gammaproteobacteria	1236	222	18	41	3	60	1	0
Other Proteobacteria	3018035	6	17	100	50	17	0	0
Spirochaetes	203692	10	40	0	50	10	75	0
Synergistetes	508458	5	40	0	0	0	40	0
Thermotogae	188708	9	56	40	0	0	78	22
Verrucomicrobia	74201	9	11	0	33	0	17	0
Other Bacteria	2*	27	30	25	15	0	26	9

*Taxonomic clades not included in iTOL trees

Table S2. DFT-computed geometric values^a for Models of $\text{cmnm}^5\text{s}^2\text{U}$ following H-atom abstraction

Model	$\text{C}_c\text{—C}_d$ (Å)	$\text{N}_b\text{—C}_c$ (Å)	$\text{C}_a\text{—N}_b$ (Å)
UHH ^b	1.533	1.487	1.508
C_c^\bullet	1.459	1.422	1.516
N_b^\bullet	1.524	1.431	1.428
C_a^\bullet	1.524	1.501	1.458
UH	1.546	1.470	1.467
C_c^\bullet	1.444	1.371	1.454
N_b^\bullet	1.855	1.372	1.450
C_a^\bullet	1.540	1.454	1.374
U	1.592	1.461	1.511
C_c^\bullet	1.486	1.384	1.445
N_b^\bullet	1.677	1.401	1.435
C_a^\bullet	1.570	1.449	1.345

- a. Bond lengths shown in blue are seen to shorten significantly upon the denoted H-atom abstraction, indicating partial double bond formation. Bond lengths shown in red are seen to lengthen indicating bond breaking.
- b. Geometric parameters listed for models named **UHH**, **UH**, and **U** are those for $\text{cmnm}^5\text{s}^2\text{U}$ models *prior* to H-atom abstraction.

Table S3. Strains and plasmids used.

Strain, plasmid	Phenotype, genotype and/or description	Ref/Source
<i>S. pneumoniae</i>		
IU1824	D39 $\text{rpsL1 } \Delta\text{cps rpsL1 spd}_{0567}(\text{mnmM})(\text{Q152stop})$	(1)
IU19821	D39 $\Delta\text{cps rpsL1 } \Delta\text{spd}_{0567}::\text{P}_c\text{-[sacB-kan-rpsL}^+]$	(2)
IU19835	D39 $\Delta\text{cps rpsL1 spd}_{0567}^+$	(2)
IU19964	D39 $\Delta\text{cps rpsL1 } \Delta[\text{spd}_{0565-0566}] (\Delta\text{ytqA})$ markerless (IU19821 X fusion $\Delta[\text{spd}_{0565-0566}]$ amplicon)	This study
IU19966	D39 $\Delta\text{cps rpsL1 } \Delta\text{spd}_{0567} (\Delta\text{mnmM})$ markerless (IU19821 X fusion Δspd_{0567} amplicon)	This study
IU19968	D39 $\Delta\text{cps rpsL1 D39 } \Delta\text{cps rpsL1 } \Delta[\text{spd}_{0565-0567}] (\Delta\text{ytqA mnmM})$ markerless (IU19821 X fusion $\Delta[\text{spd}_{0565-0567}]$ amplicon)	This study
IU19974	D39 $\Delta\text{cps rpsL1 } \Delta\text{spd}_{0567} (\Delta\text{mnmM})$ markerless// $\Delta\text{bgaA}::\text{kan-t1t2-P}_{\text{Zn}}\text{-mnmM}^+$ (IU19966 X fusion $\Delta\text{bgaA}::\text{kan-t1t2-P}_{\text{Zn}}\text{-mnmM}^+$)	This study
<i>B. subtilis</i>		
CU1065	Wild-Type, $\text{trpC2 attSP}\beta \text{ sfp0}$	Laboratory Stock
BKE30480	CU1056 $\Delta\text{ytqA}::\text{Erm}^R$	(3)
BKE30490	CU1056 $\Delta\text{mnmM}::\text{Erm}^R$	(3)
<i>S. mutans</i>		

S. mutans UA159	Serotype c, ATCC 700610	(4)
MSJ1093	<i>S. mutans</i> UA159 Δ ytqA::Erm ^R	This study
MSJ1095	<i>S. mutans</i> Δ ymnmM::Erm ^R	This study
MSJ1097	<i>S. mutans</i> Δ ytqA mnmM::Erm ^R	This study
<i>E. coli</i>		
JW5380-2	Δ (araD-araB)567, Δ lacZ4787(::rrnB-3), λ , Δ trmC732::kan, rph-1, Δ (rhaD-rhaB)568, hsdR514	(5)
TOP10	F- mcrA Δ (mrr-hsdRMS-mcrBC) ϕ 80 lacZ Δ M15 Δ lacX74 recA1 ara Δ 139 Δ (ara-leu)7697 galU galK rpsL (StrR) endA1 nupG	Invitrogen
Plasmids		
pBAD pBAD/Myc-His	Amp ^R , ColE1 arabinose inducible promoter	(6)
pDS358	pBAD-ytqA _{Bsu}	This study
pDS359	pBAD-ytqA _{Bsu}	This study
pDS365	pBAD-ytqB _{Bsu}	This study

Table S4. Oligonucleotides used

Oligo	Sequence 5' - 3'
For construction of MSJ1093	
ytqA P1	GCAGTGATTGCTTTAGTTGTCC
ytqA P2	GCGCGCTGCAGACAAAAAGTACAGCCACCATGA
ytqA P3	GCGCGGAGCTCTCATTATCGTCTGACAGGTGA
ytqA P4	ATCCTCCTCTCGTAGAGGTA
For construction of MSJ1095	
ytqB P1	GTGATGGAAGTGTGGCTCATG
ytqB P2	GCGCGCTGCAGGGCCTGTTCTGTACATCAAAA
ytqB P3	GCGCGGAGCTCGGGTGGCGATAAGGAAAAAGAT
ytqBP4	AGTCAAAAAGGGAGAAAATTGGGT
For construction of MSJ1097	
ytqAB P1	GCAGTGATTGCTTTAGTTGTCC
ytqAB P2	GCGCGCTGCAGCGTACAAAAAGTACAGCCACCA
ytqAB P3	GCGCGGAGCTCGGGTGGCGATAAGGAAAAAGAT
ytqAB P4	AGTCAAAAAGGGAGAAAATTGGGT
For verification of MSJ1062 and MSJ1063	
BSU_ytqB_VF	CAAAGAAGTGTGAAAATGGCC
BSU_ytqB_VR	TGCTGATTGATAAACCCGTATGT
BSU_ytqA_VF	GCACGAAAAATGGAAGGACG
BSU_ytqA_VR	GCCGTGTTTTCTTAATTTATTGACG
For verification of MSJ1093, MSJ1095, and MSJ1097	
SMU_ytqA_VF	CCAGTGTGTTAACTGGAATCAC
SMU_ytqA_VR	AGTCGCATCAATGGCTATACTG
SMU_ytqB_VF	CATTCATCGTCTGACAGGTGA

SMU_ytqB_VR	ATCCTCCTCCTTCGTAGAGGTA
For construction of IU19964	
TT1519	GGCATGATAGAAGGCGTAGAAGTGATGTTCTCC
TT1618	TTACAGCCTTGCATCCTTGAACACTTCCTTCTCCAAAGAGTTTTCGATAATAATCATT
TT1619	AATGATTATTATCGAAAACCTTTGGAGAAGGAAGTGTTCAAGGATGCAAGGCTGTAA
TT1520	CCAGAAGCATCATTCAAGAGTCCTTCGCCC
For construction of IU19966	
TT1522	GTCCCTATTGATGCGGAATTTGACTGTCCC
TT1623	AATCATCACTAAAAACGGCGGGTTGTTGACTCCCATAGTCGCATCCACTACGACATCCT C
TT1624	GAGGATGTCGTAGTGGATGCGACTATGGGAGTCAACAACCCGCCGTTTTTAGTGATGA TT
TT1520	CCAGAAGCATCATTCAAGAGTCCTTCGCCC
For construction of IU19968	
TT1519	GGCATGATAGAAGGCGTAGAAGTGATGTTCTCC
TT1621	ATCATCACTAAAAACGGCGGGTTGTTGACTTCTCCAAAGAGTTTTCGATAATAATCATT
TT1622	AATGATTATTATCGAAAACCTTTGGAGAAGTCAACAACCCGCCGTTTTTAGTGATGAT
TT1520	CCAGAAGCATCATTCAAGAGTCCTTCGCCC
For construction of IU19974	
TT657	CGCCCCAAGTTCATACCAATGACATCAAC
TT1577	TGCCATCTCAAGTGGTCTTTTCATTTTCAATACATCGCTTCTCTCTATCTTCCTTGTTA
TT1578	TAACAAGGAAGATAGAGAGGAAGCGATGTATTGAAAATGAAAAGACCACTTGAGATG GCA
TT1579	ACTGGTTTATGAGAAAGTAAGTTCTTTTATCCATGTCTGTATCTCTCTAATTTTTCAATC
TT1580	AAAAATTAGAGAGATACAGACATGGATAAAAGAACTTACTTTCTCATAAACCAAGTTGCT G
CS121	GCTTTCTTGAGGCAATTCACCTGGTGC
For Construction of pBAD24 Complementation Vectors	
YtqA_NcoI_F	GTACCATGGAGAACAATCCTTTTCCTTATTCAAATAC
YtqA_XhoI/BamHI_R	ACTGGATCCTCACTCGAGCGCTGATTCCTCCTCAAGCCG
YtqB_BamHI_R	GACTGGATCCTCATTTGCTGATCTGAGCTTTT
YtqB_NcoI_F	GTACCATGGTTTTGAAGAAAATTCTTCCTTACAGCAA

Table S5. Buffer gradient used in the LC-MS/MS Method 2. Buffer A: 0.02% Formic acid in double distilled water. Buffer B: 0.02% Formic acid in 70% Acetonitrile.

Time (min)	Buffer A (%)	Buffer B (%)	Flow (ml/min)
0	100	0	0.3
5	99	1	0.3
6	98	2	0.3
7	97	3	0.3
8	95	5	0.3
9	93	7	0.3
10	90	10	0.3
12	88	12	0.3
13	85	15	0.3
15	80	20	0.3
16	25	75	0.3
17	0	100	0.3
18	0	100	0.3
20	0	100	0.3
21	100	0	0.3
25	100	0	0.3

Table S6. Identifiers for proteins and genomes used in Fig. S4 and S5

YtqA_Name in FigS4A	Genome	Genome ID	Accession	BRC ID	RefSeq Locus Tag	Protein ID	AA length
N_Spneumoniae_ST556	Streptococcus pneumoniae ST556	1130804.3	CP003357	fig 1130804.3.peg.715	MY_0697	AFC94358.1	169
C_Spneumoniae_ST556	Streptococcus pneumoniae ST556	1130804.3	CP003357	fig 1130804.3.peg.716	MY_0698	AFC94359.1	64
N_Spneumoniae_TIGR4	Streptococcus pneumoniae TIGR4	170187.11	NC_003028	fig 170187.11.peg.680			169
C_Spneumoniae_TIGR4	Streptococcus pneumoniae TIGR4	170187.11	NC_003028	fig 170187.11.peg.681			148
N_Spneumoniae_R6	Streptococcus pneumoniae R6	171101.6	NC_003098	fig 171101.6.peg.635	spr0569	NP_358163.1	150

C_Spneumoniae_R6	Streptococcus pneumoniae R6	171101.6	NC_003098	fig 171101.6.peg.636	spr0570	NP_358164.1	148
N_Spneumoniae_D39	Streptococcus pneumoniae D39	373153.27	NC_008533	fig 373153.27.peg.643	SPD_0565	YP_816064.1	150
C_Spneumoniae_D39	Streptococcus pneumoniae D39	373153.27	NC_008533	fig 373153.27.peg.644	SPD_0566	YP_816065.1	148
Smitis_OT25	Streptococcus mitis strain OT25	28037.212	JYGP01000002	fig 28037.212.peg.409	TZ90_00447	KJQ68083.1	318
Smutans_UA159	Streptococcus mutans UA159	210007.7	NC_004350	fig 210007.7.peg.1517	SMU.1699c	NP_722028.1	310
MnmM_Name in FigS4A							
Spneumoniae_ST556	Streptococcus pneumoniae ST556	1130804.3	CP003357	fig 1130804.3.peg.717	MYY_0699	AFC94360.1	185
Spneumoniae_TIGR4	Streptococcus pneumoniae TIGR4	170187.11	NC_003028	fig 170187.11.peg.682	SP_0652	NP_345157.1	185
Spneumoniae_R6	Streptococcus pneumoniae R6	171101.6	NC_003098	fig 171101.6.peg.637	spr0571	NP_358165.1	185
Smutans_UA159	Streptococcus mutans UA159	210007.7	NC_004350	fig 210007.7.peg.1516	SMU.1697c	NP_722027.1	181
Smitis_OT25	Streptococcus mitis strain OT25	28037.212	JYGP01000002	fig 28037.212.peg.410	TZ90_00448		185
Spneumoniae_D39	Streptococcus pneumoniae D39	373153.27	NC_008533	fig 373153.27.peg.645	SPD_0567	YP_816066.1	185

Supplemental Figures

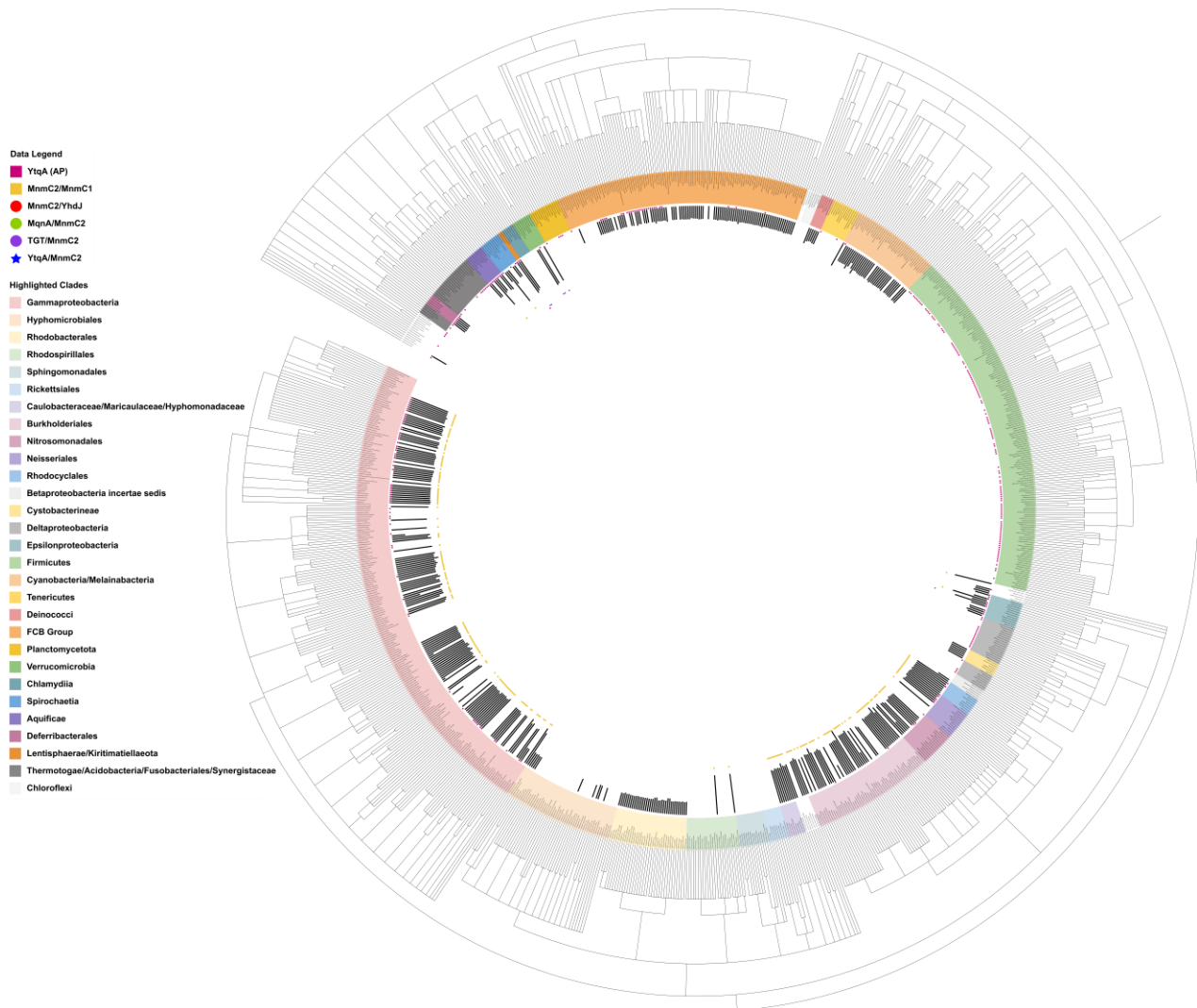


Figure S1. Distribution of MnmC2 and MnmC2 fusions in the bacterial COG database genomes. The presence of MnmC2 is represented by the respective homologs' lengths shown by the black histograms (2nd row, from outside-in) (**Supplemental data S3**). YtqA absence-presence is also shown by the fuchsia squares (1st row, outside-in). MnmC2/MnmC1 fusions are denoted by the goldenrod squares (3rd row). MnmC2/YhdJ fusions were noted by red circles (7th row) and MqnA(MqnD)/MnmC2 fusions by green circles (4th row), while the TGT/MnmC2 and YtqA/MnmC2 fusions were denoted by purple circles (5th row) and blue stars (6th row), respectively (derived from fusion data, **Supplemental data S3 and S4**). Clades of interest are highlighted in various colors across leaf labels, the key to which is provided left of the figure. An interactive version of this tree can be accessed at <https://itol.embl.de/tree/8216522107187281668281889>.

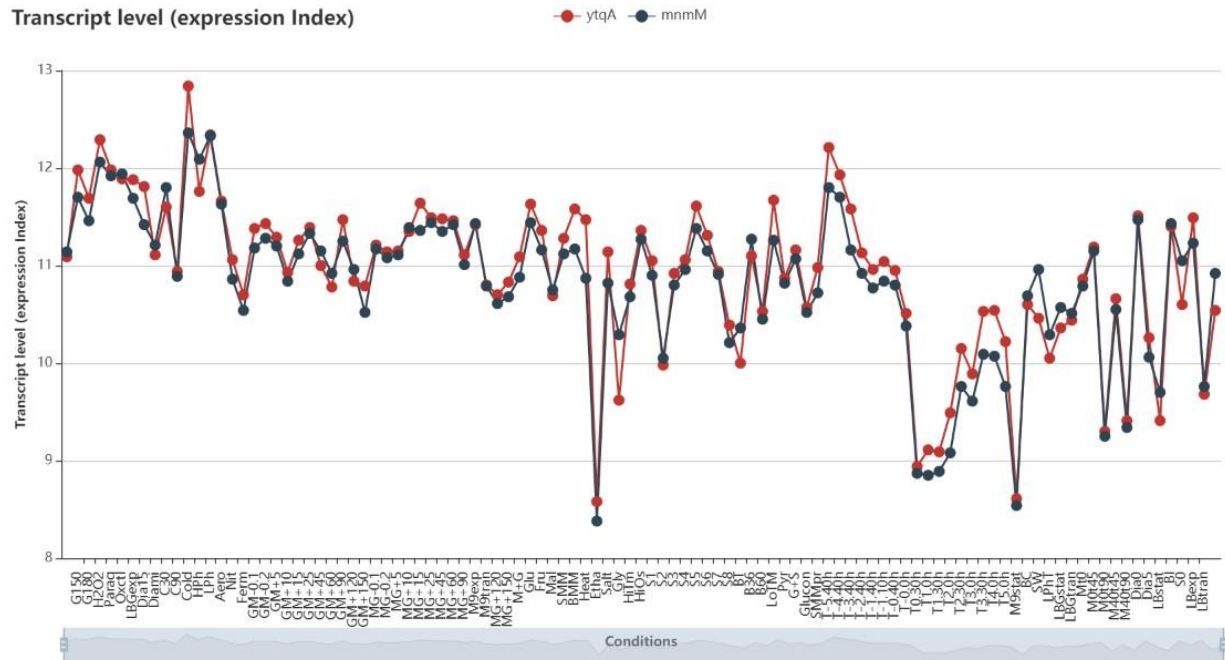


Figure S2. Coexpression of YtgA and YtgB/MnmM in *B. subtilis*. Data extracted from SubtiWiki <http://subtiwiki.uni-goettingen.de/> expression browser using BSU_30480 (*ytqA*) and BSU_30490 (*mnmM*) as inputs.

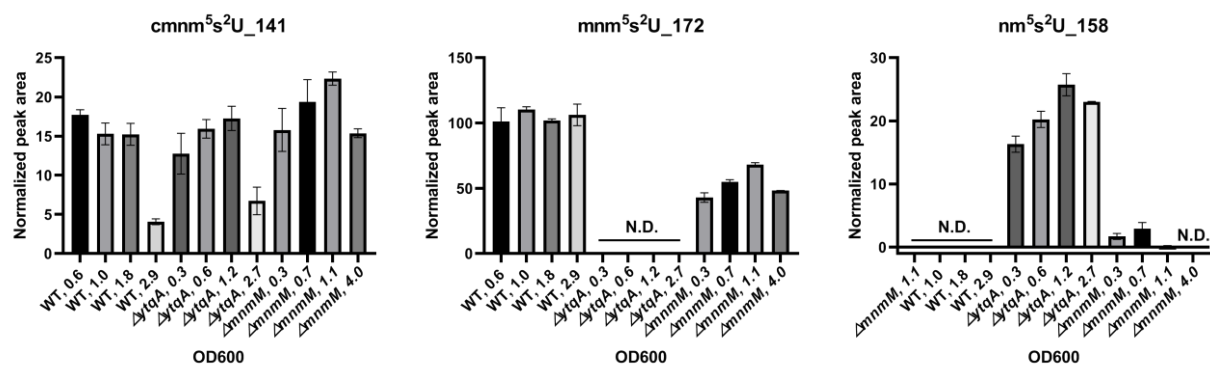
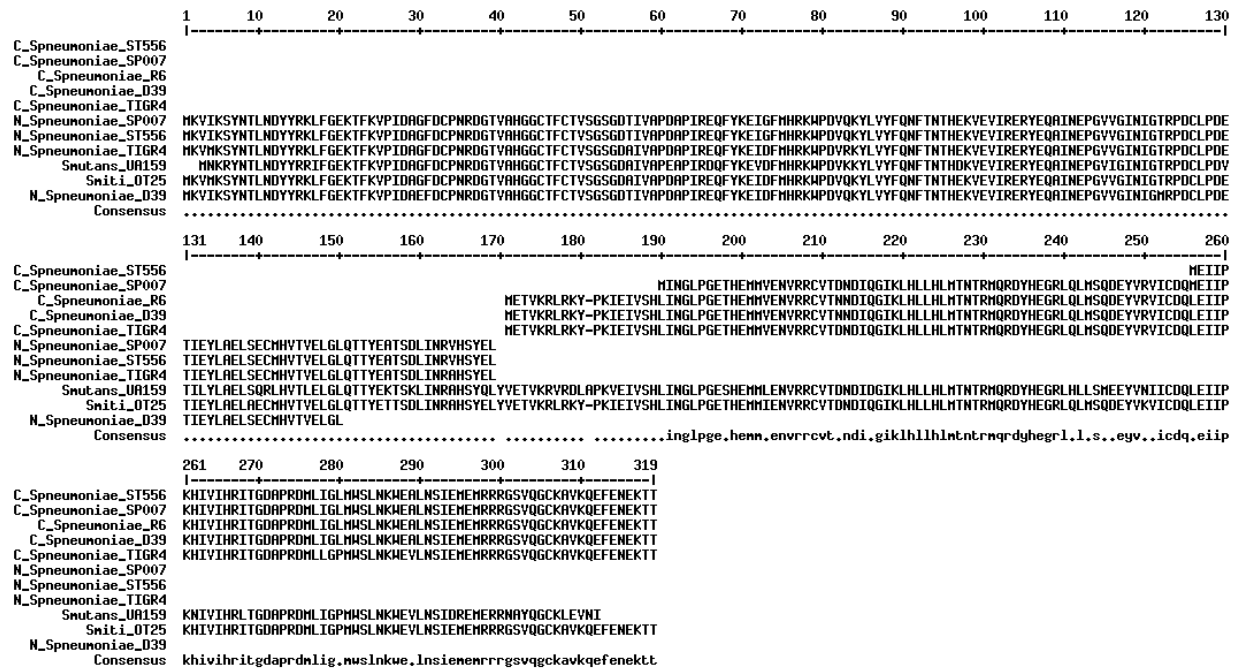


Figure S3. Analysis of xm⁵s²U profiles in *Bacillus subtilis* WT and *ytqA* and *mnmM* mutant strains. Normalized peak area values for cmnm⁵s²U, mnm⁵s²U and nm⁵s²U. The modification signals were based on specific transitions (cmnm⁵s²U_141, mnm⁵s²U_172 and nm⁵s²U_158) and were confirmed by both qualifier and quantifier transitions; 200 ng of hydrolysate was injected. tRNA samples were processed through VDCL2 method and analyzed through LC-MS method 2 as described in the methods section. N.D., Not detected. Samples were extracted at different stages of growth with OD (A_{600nm}) ranging from 0.3 to 4. Data represent the mean ±SD for 2 technical replicates.

A



B

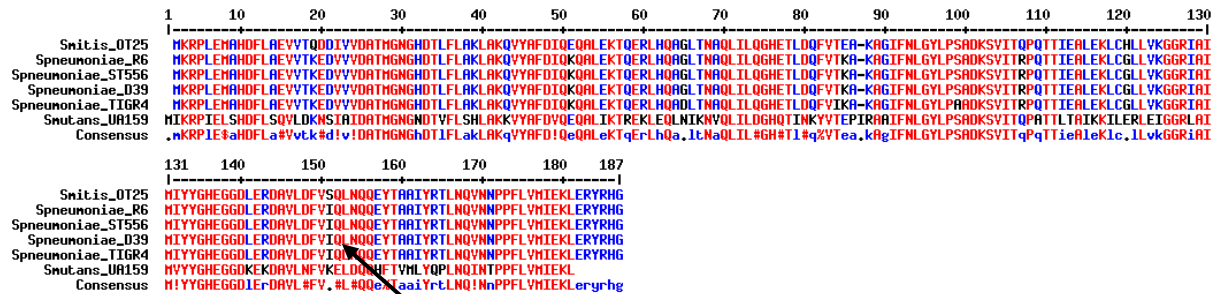


Figure S4. Sequence similarities of YtqA orthologs. **(A)** Alignments of truncated YtqA proteins from different *S. pneumoniae* strains (N-terminal and C-terminal halves are noted by a “C” or and an “N” in front of the species name) with full-length YtqA sequence from *S. mutans* (SMU_1699c) and *S. mitis* (TZ90_00447) using MultiAlin with default parameters. **(B)** Alignment of MnmM sequences from different *S. pneumoniae* strains with *S. mutans* (SMU_1697) and *S. mitis* (TZ90_00448) homologs. The location of the Q152STOP mutation that occurred in the IU1824 strain is shown with an arrow. Identifiers for all proteins in the alignments are listed in **Table S6**.

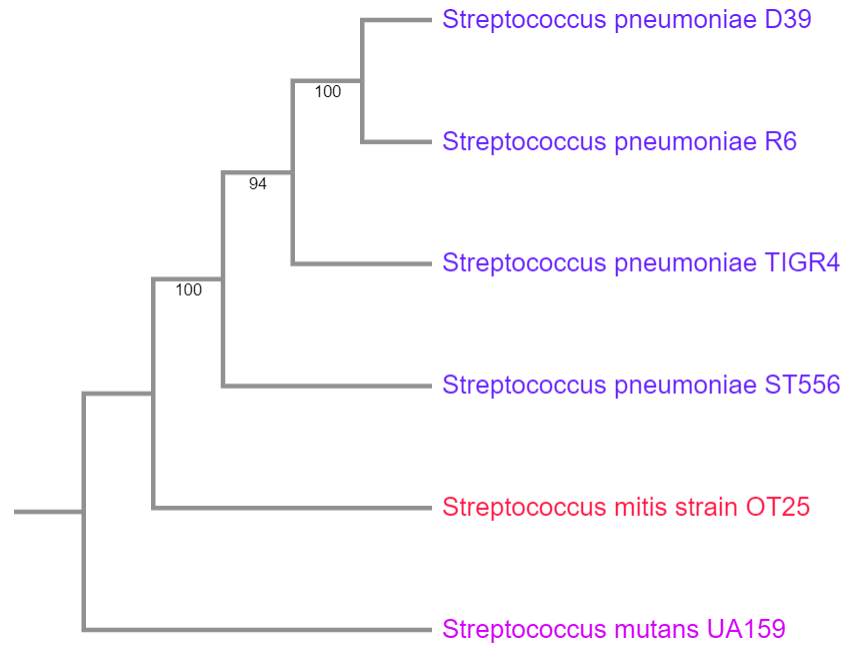
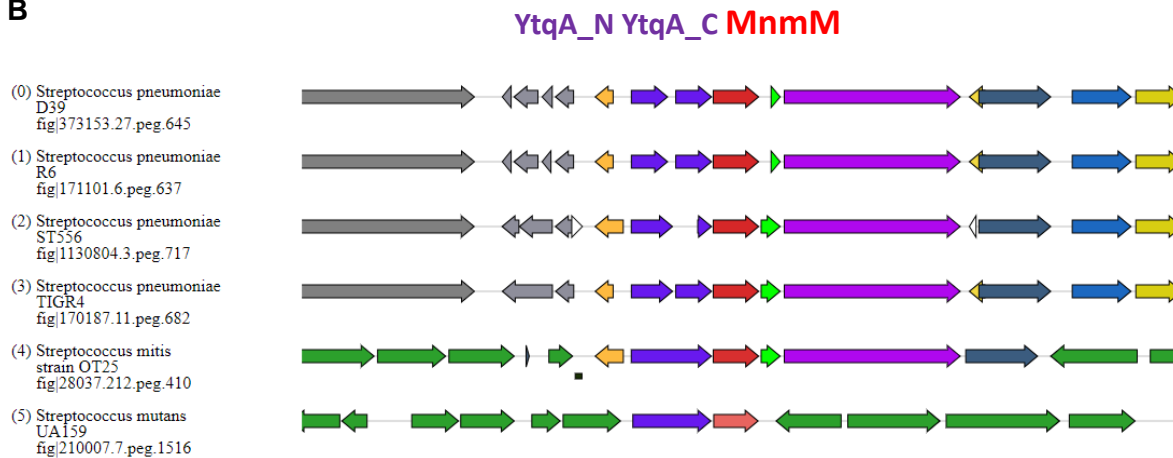
A**B**

Figure S5. Diversity of *Streptococci* mnm^{5s2U} biosynthetic genes. **(A)** The species tree shows the relationship between the *S. pneumoniae*, *S. mutans*, and *S. mitis* strains discussed in this study. The tree was built using BV-BRC bacterial Phylogenetic Tree Service that used the Codon Tree method that selects single-copy BV-BRC PGFams and analyzes aligned proteins and coding DNA from single-copy genes using the program RAXML (7). **(B)** Gene neighborhoods generated using Gizmogene around the *mnmM* (in red) genes from the genomes shown in (A), showing the full-length or truncated *ytqA* (*ytqA_N* and *ytqA_C* genes (in purple). Identifiers for all genomes and genes are given in **Table S6**.

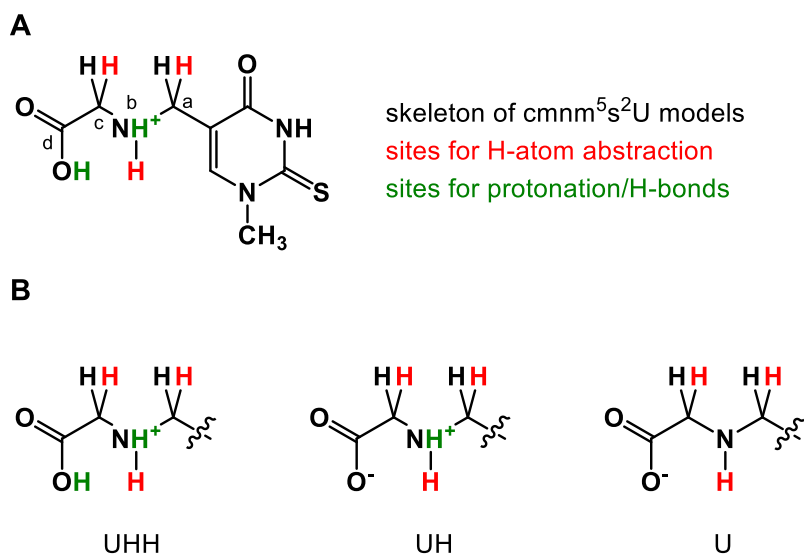
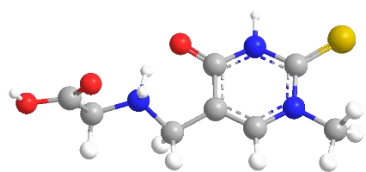
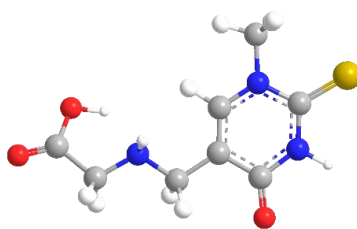


Figure S6. Models of $\text{cmnm}^5\text{s}^2\text{U}$ employed in DFT calculations. Three different protonation states were considered (sites shown in green): UHH, where the carboxylate and amide functional groups of the pendant glycine are protonated; UH, in which only the amide is protonated; and U, in which neither group is protonated. Three sites for H-atom abstraction were considered (sites shown in red): the glycine alpha carbon (C_c); the amide nitrogen (N_b); and the ^5U -methylene carbon (C_a).



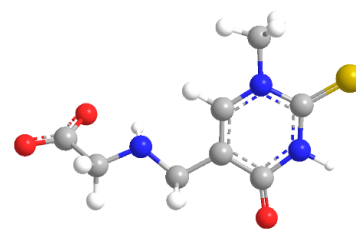
UHH

atom	x (Å)	y (Å)	z (Å)
C(1)	0.211	0.533	-0.651
C(2)	0.335	1.318	0.570
C(3)	1.489	1.189	1.311
O(4)	-0.769	0.611	-1.431
N(5)	1.277	-0.300	-0.923
C(6)	-0.859	2.135	0.996
N(7)	2.511	0.349	0.969
C(8)	3.717	0.264	1.809
C(9)	2.451	-0.466	-0.183
S(10)	3.643	-1.509	-0.640
N(11)	-1.485	2.765	-0.222
C(12)	-2.847	3.342	-0.073
C(13)	-2.858	4.658	-0.860
O(14)	-4.077	5.177	-0.946
O(15)	-1.830	5.133	-1.312
H(16)	1.641	1.758	2.242
H(17)	1.222	-0.866	-1.780
H(18)	-0.601	2.919	1.734
H(19)	-1.643	1.486	1.443
H(20)	4.609	0.540	1.214
H(21)	3.854	-0.775	2.165
H(22)	3.600	0.951	2.666
H(23)	-1.426	1.937	-0.949
H(24)	-0.901	3.549	-0.608
H(25)	-3.067	3.558	0.994
H(26)	-3.621	2.642	-0.443
H(27)	-4.026	6.030	-1.438



UH

atom	x (Å)	y (Å)	z (Å)
C(1)	-0.059	-0.800	-0.077
C(2)	-0.059	0.662	0.060
C(3)	1.121	1.292	0.349
O(4)	-1.036	-1.496	-0.342
N(5)	1.214	-1.376	0.127
C(6)	-1.373	1.370	-0.158
N(7)	2.323	0.633	0.532
C(8)	3.538	1.390	0.848
C(9)	2.415	-0.756	0.423
S(10)	3.833	-1.607	0.629
N(11)	-1.374	2.749	0.345
C(12)	-2.593	3.524	0.073
C(13)	-2.264	5.027	-0.079
O(14)	-3.102	5.901	-0.041
O(15)	-0.952	5.240	-0.298
H(16)	1.169	2.387	0.449
H(17)	1.264	-2.397	0.040
H(18)	-2.178	0.734	0.283
H(19)	-1.595	1.402	-1.249
H(20)	4.307	1.221	0.070
H(21)	3.961	1.047	1.813
H(22)	3.280	2.463	0.903
H(23)	-0.567	4.314	-0.238
H(24)	-1.193	2.738	1.359
H(25)	-3.401	3.410	0.828
H(26)	-3.021	3.194	-0.898



U

atom	x (Å)	y (Å)	z (Å)
C(1)	-0.025	-0.762	-0.345
C(2)	-0.109	0.648	0.029
C(3)	1.017	1.272	0.493
O(4)	-0.929	-1.481	-0.770
N(5)	1.279	-1.303	-0.156
C(6)	-1.413	1.405	-0.071
N(7)	2.251	0.648	0.633
C(8)	3.400	1.409	1.122
C(9)	2.422	-0.688	0.309
S(10)	3.881	-1.511	0.459
N(11)	-1.253	2.798	0.257
C(12)	-2.466	3.609	0.331
C(13)	-2.185	5.001	-0.389
O(14)	-3.031	5.902	-0.203
O(15)	-1.127	5.001	-1.096
H(16)	0.937	2.328	0.800
H(17)	1.388	-2.293	-0.397
H(18)	-2.136	0.920	0.629
H(19)	-1.847	1.197	-1.091
H(20)	4.218	1.392	0.374
H(21)	3.796	0.955	2.052
H(22)	3.074	2.448	1.308
H(23)	-0.732	3.334	-0.491
H(24)	-2.802	3.801	1.376
H(25)	-3.334	3.142	-0.202

Figure S7. Geometry optimized models and xyz coordinates (Å) of $cmnm^5s^2U$ that were further geometry-optimized after H-atom abstraction.

Supplemental data description

Data S1

List of the 968 organisms in the COG database that encode the three proteins MnmA, MnmG and MnmE and distribution of the COG4121(MnmC) in those genomes.

Data S2

Summary of MnmC1/MnmC2/MnmC1C2 distributions across bacterial orders in the benchmark set of 968 genomes.

Data S3

Domain analysis of MnmC1/MnmC2/MnmC1C2 (via CDD Search) in homologs present in benchmark set of 968 genomes

Data S4

(a) List of YtqA/mnmM, MnmC1/MnmM and YtqA/MnmC2 fusion proteins present in InterPro; (b) YtqA/YhcC family proteins found in the benchmark set of 968 genomes.

Data S5

YtqA/YhcC gene clusters (a) all, (b) those with mnmM. YtqAs taken from initial COG Db fusion analysis) (c) YtqA/YhcC-physically clustered gene analyses identifying methylase/methyltransferase domains via three methods, results in numeric form (1, BLASTp; 2, CDD Search; 3, InterProScan); (d) YtqA-physically clustered gene analyses identifying methylase/methyltransferase domains via three methods, results with all hit sequence identifiers (1, BLASTp; 2, CDD Search; 3, InterProScan); (e) summary metrics for different methods determining methylase/methyltransferase domains among genes physically-clustered with YtqA/YhcC

Data S6

MnmC1/MnmC2/MnmC1C2, and physically clustered YtqA-MnmM occurrence data across bacterial orders. Data for each set of sequences includes the incidence counts across genomes and the calculated frequency for each bacterial order. These different sets of data was used to generate Fig. 2. All column counts/percentages were determined independently of each other, and, therein, MnmC1 and MnmC2 counts could be part of fusions or non-fused free-standing domains (*factually, however, the latter is not the case for MnmC1 as its occurrence was always observed in the form of a fusion).

Data S7

Differential YtqA gene cluster, MnmC1/MnmC2/MnmC1C2 fusion analysis data summary tables. For organisms containing YtqA from the benchmark genome set (filtered for positive MnmAGE status), the distributions of retrieved YtqA gene cluster data across genomes of select MnmC1/MnmC2/MnmC1C2 encoding statuses (subtables are labeled with their respective genome statuses).

Data S8

Complete YtqA/YhcC gene cluster, MnmC1/MnmC2/MnmC1C2 fusion analysis data mapping to SSN Figure: (a) "Node Count Cluster Number" mapped to "Sequence Count Cluster Number" for SSN mapping;"Node Count Cluster Number" is the actual cluster number within the SSN figure (follows visual order of appearance from top-left to bottom-right). (b) YtqA/YhcC gene cluster data mapped to an exported table of the AS100 reptime 55 YtqA/YhcC family SSN. (c) YtqA/YhcC gene cluster data-to-SSN cluster mapped data master sheet. (d) SSN-mapped YtqA/YhcC gene cluster data was transformed relative to unique metabolic category per gene cluster; data was used in subsequent metabolic category and gene symbol/family name analyses. (e) Taxonomic group distributions YtqA/YhcC gene clusters, MnmC1/MnmC2/MnmC1C2 fusion analysis data mapping to SSN. (f) Taxonomic group distributions YtqA/YhcC gene clusters, MnmC1/MnmC2/MnmC1C2 fusion analysis data mapping to SSN expanded relative to SSN cluster numbers.

Data S9

SSN file available in the FigShare depository: <https://doi.org/10.6084/m9.figshare.25403692.v1>.

References

1. Lanie JA, Ng WL, Kazmierczak KM, Andrzejewski TM, Davidsen TM, Wayne KJ, Tettelin H, Glass JI, Winkler ME. 2007. Genome sequence of Avery's virulent serotype 2 strain D39 of *Streptococcus pneumoniae* and comparison with that of unencapsulated laboratory strain R6. *J Bacteriol* 189:38-51
2. Tsui HCT, Joseph M, Zheng JJ, Perez AJ, Manzoor I, Rued BE, Richardson JD, Branny P, Doubravová L, Massidda O, Winkler ME. 2023. Negative regulation of MurZ and MurA underlies the essentiality of GpsB- and StkP-mediated protein phosphorylation in *Streptococcus pneumoniae* D39. *Mol Microbiol* 120:351-383.
3. Koo B-M, Kritikos G, Farelli JD, Todor H, Tong K, Kimsey H, Wapinski I, Galardini M, Cabal A, Peters JM, Hachmann A-B, Rudner DZ, Allen KN, Typas A, Gross CA. 2017. Construction and analysis of two genome-scale deletion libraries for *Bacillus subtilis*. *Cell Syst* 4:291-305.e7.
4. Ajdić D, McShan WM, McLaughlin RE, Savić G, Chang J, Carson MB, Primeaux C, Tian R, Kenton S, Jia H, Lin S, Qian Y, Li S, Zhu H, Najjar F, Lai H, White J, Roe BA, Ferretti JJ. 2002. Genome sequence of *Streptococcus mutans* UA159, a cariogenic dental pathogen. *Proc Natl Acad Sci U S A* 99:14434-9
5. Baba T, Ara T, Hasegawa M, Takai Y, Okumura Y, Baba M, Datsenko KA, Tomita M, Wanner BL, Mori H. 2006. Construction of *Escherichia coli* K-12 in-frame, single-gene knockout mutants: the Keio collection. *Mol Syst Biol* 2:2006.0008.
6. Guzman LM, Belin D, Carson MJ, Beckwith J. 1995. Tight regulation, modulation, and high-level expression by vectors containing the arabinose PBAD promoter. *J Bacteriol* 177:4121-4130.
7. Olson RD, Assaf R, Brettin T, Conrad N, Cucinell C, Davis JJ, Dempsey DM, Dickerman A, Dietrich EM, Kenyon RW, Kuscuoglu M, Lefkowitz EJ, Lu J, Machi D, Macken C, Mao C, Niewiadomska A, Nguyen M, Olsen GJ, Overbeek JC, Parrello B, Parrello V, Porter JS, Pusch GD, Shukla M, Singh I, Stewart L, Tan G, Thomas C, VanOeffelen M, Vonstein V, Wallace ZS, Warren AS, Wattam AR, Xia F, Yoo H, Zhang Y, Zmasek CM, Scheuermann RH, Stevens RL. 2023. Introducing the Bacterial and Viral Bioinformatics Resource Center (BV-BRC): a resource combining PATRIC, IRD and ViPR. *Nucleic Acids Res* 51:D678-D689.